Increasing the Temporal Resolution of Direct Normal Solar Irradiance Forecasted Series

Carlos M. Fernández-Peruchena[1, a)], Martin Gastón[2], Marion Schroedter-Homscheidt[3], Isabel Martínez Marco[4], José L. Casado-Rubio[4], José Antonio García-Moya[4]

[1] *National Renewable energy Centre (CENER), C/ Isaac Newton n 4 - Pabellón de Italia, 41092 Seville, Spain. Tel.: (+34) 902 25 28 00*
[2] *CENER,* [3] *German Aerospace Center (DLR),* [4] *Agencia Estatal de Meteorología (AEMET)*

[a)] Corresponding author: cfernandez@cener.com

Abstract. A detailed knowledge of the solar resource is a critical point in the design and control of Concentrating Solar Power (CSP) plants. In particular, accurate forecasting of solar irradiance is essential for the efficient operation of solar thermal power plants, the management of energy markets, and the widespread implementation of this technology. Numerical weather prediction (NWP) models are commonly used for solar radiation forecasting. In the ECMWF deterministic forecasting system, all forecast parameters are commercially available worldwide at 3-hourly intervals. Unfortunately, as Direct Normal solar Irradiance (DNI) exhibits a great variability due to the dynamic effects of passing clouds, 3-h time resolution is insufficient for accurate simulations of CSP plants due to their nonlinear response to DNI, governed by various thermal inertias due to their complex response characteristics. DNI series of hourly or sub-hourly frequency resolution are normally used for an accurate modeling and analysis of transient processes in CSP technologies. In this context, the objective of this study is to propose a methodology for generating synthetic DNI time series at 1-h (or higher) temporal resolution from 3-h DNI series. The methodology is based upon patterns as being defined with help of the clear-sky envelope approach together with a forecast of maximum DNI value, and it has been validated with high quality measured DNI data.

INTRODUCTION

The nonlinear influence of Direct Normal solar Irradiance (DNI) on the efficiency of concentrating solar power (CSP) plants and the controllability of power generation through thermal energy storage (if available), makes the DNI forecasts especially important for the management and operation of these plants and the widespread implementation of this technology.

The selection of a particular solar irradiance forecasting methodology is heavily dependent on the timescale involved, which ranges from intra-hour to few days ahead horizons. Different time horizons are relevant according to the forecast application. In particular, intraday forecasts are useful for load following and pre-dispatch, reducing the need for frequency control ("regulation") in "real" time, whereas day-ahead solar forecasts (<48 hours) are useful for energy resource planning and scheduling [1]. Intrahour and intraday forecasting is usually addressed by stochastic-learning and sky-imaging based approaches.

Numerical weather prediction (NWP) models describe atmospheric physical processes (pressure, wind, temperature, water-vapor condensation/evaporation, and radiative transfer of solar and longwave radiation). These models can be used to propagate forward the current state of the atmosphere (initial conditions) with the aim of obtaining a forecast for future weather. The state of the atmosphere is described by the spatial distribution of wind,

SolarPACES 2016
AIP Conf. Proc. 1850, 140007-1–140007-8; doi: 10.1063/1.4984515
Published by AIP Publishing. 978-0-7354-1522-5/$30.00

temperature, and other weather variables. It is worth to mention that non-linear equations describing the evolution of the atmosphere do not have analytical solutions. Hence, NWP models are generally performed by numerical integration of the hydrodynamic equations governing atmospheric motions. With the introduction of powerful computers in meteorology, the meteorological community has invested more time and efforts to develop more and more complex numerical models of the atmosphere. Unfortunately, there are great shortcomings in the description of the initial state of the atmosphere. The initial conditions of any numerical integration are given by very complex assimilation procedures which estimate the state of the atmosphere by considering all available observations. The fact that a limited number of observations are available (compared to the degrees of freedom of the system) and that part of the globe is characterized by a very poor coverage introduces uncertainties in the initial conditions.

NWP models are commonly used for solar radiation forecasting as they provide an overall and low frequency understanding of solar forecasting. Unfortunately, DNI is influenced by events that are very difficult to forecast, in particular passing clouds and aerosol dynamics (including wildfires, dust storms, and episodic air pollution events). Also, NWP models are unable to cover a local statistical representativeness of the DNI high frequency dynamics as a consequence of the high variability of atmospheric phenomena involved (mainly passing clouds). On the other hand, purely stochastic methods (based on nonlinear interactions between variables instead a physical model per se) cover statistical behavior but may not necessarily yield an explicit model for all of the physical relationships involved. Consequently, there is a significant potential to improve the NWP models forecast performance by combining them with local high frequency DNI dynamics.

In the ECMWF deterministic forecasting system, all forecast parameters are commercially available worldwide at 3-hourly intervals. Unfortunately, the use of low frequency DNI series filters out their shorter time-scale intermittencies which influence the management and integration of power output from CSP plants. Consequently, 3-h time resolution is insufficient for accurate simulations of CSP plants due to their nonlinear response to DNI which is governed by various thermal inertias with their complex response characteristics. DNI series of sub-hourly frequency resolution are normally used for an accurate modeling and analysis of transient processes in CSP technologies.

In this work, we present a novel approach for statistical post-processing of 3-h DNI series that dynamically assemble site information to provide high frequency DNI series. Site information is obtained from local ground measurements, and the procedure allows increasing the temporal resolution of input series up to the temporal resolution of these measurements. The methodology followed is based upon the clear-sky envelope approach together with the forecast of a theoretical maximum DNI value which acts as a threshold, and it has been validated with high quality measured DNI data.

METHODS

Measured Data

The DNI data set reported in this study has been taken from the Carpentras station of the Baseline Surface Radiation Network (BSRN, [2]) (Table 1). This global network measures surface radiative fluxes at the highest possible accuracy with well-calibrated state of-the-art instrumentation at selected sites in the major climate zones.

TABLE 1. Radiometric station selected for this study.

Station	Latitude (º)	Longitude (º)	Elevation (m)	Period
Carpentras	44.0830 N	5.0590 E	100	2005-2011

DNI dataset was measured in this station by a Kipp & Zonen CH1 Pyrheliometer, and Global Horizontal solar Irradiance (GHI) dataset was collected in this station by a Kipp & Zonen CM21 pyranometer. Solar irradiance is sampled at 1 Hz with a 1-min averaging time [2]. A stringent calibration, characterization and quality control were applied on all the data by the person in charge of the measurements to assure high accuracy as well as homogeneity in the data. Measured values were checked visually, in addition to the quality tests provided by the BSRN. The measurement period selected corresponds to seven consecutive years, which includes approximately $3.7 \cdot 10^6$ 1-min DNI values.

Experimental Procedure

First, an analysis of measured ground data is carried out to characterize patterns at 1-min time resolution. The years used for characterizing the high frequency DNI patterns at the location were the first two years of the selected period: 2005 and 2006. Pattern characterization is achieved by the non-dimensionalization of measured DNI curves in time and amplitude through a recently developed technique based on the envelope approach [3, 4]. This non-dimensionalization technique makes the transformation of high-frequency measured daily solar DNI curves possible for the generation of new daily curves of high-frequency solar DNI data. The steps followed in the construction of the synthetic series are detailed below:

- The non-dimensionalization of the temporal scale is achieved by dividing the elapsed Universal Time (UT) since sunrise by the total elapsed UT from sunrise to sunset.
- The non-dimensionalization of the DNI amplitude is achieved by dividing each actual DNI value by the corresponding DNI value of the clear-day DNI (envelope) curve.

Within this nondimensionalization scheme, every daily high-frequency DNI curve is transformed into a dimensionless curve where both the dimensionless time and irradiance scales go from 0 to 1 (Fig. 1). These curves describe Dynamic Paths in a non-dimensional space, which can be dimensionalized for predicting actual high-frequency DNI dynamics.

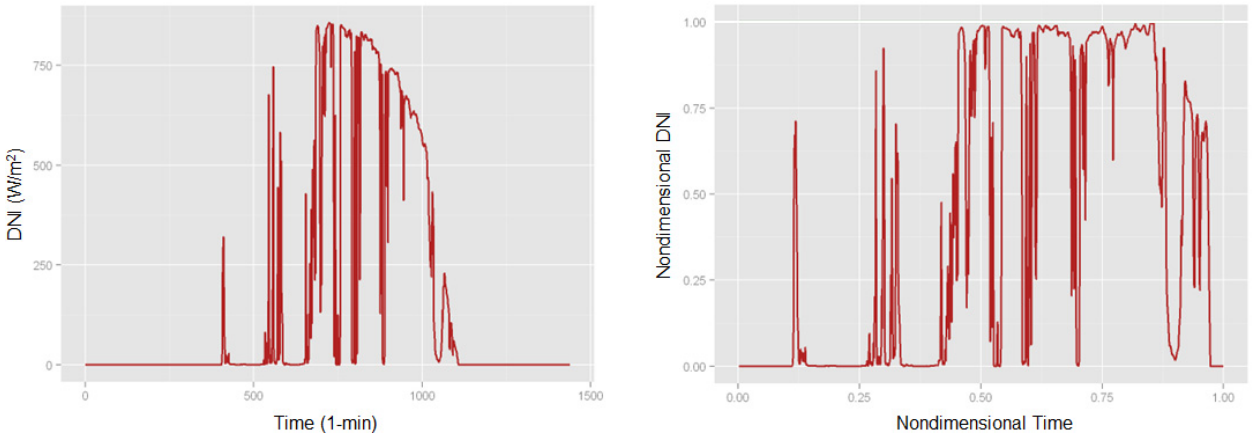

FIGURE 1. Measured DNI at Carpentras station (2016/08/20), left, with its corresponding nondimensional curve, right.

The methodology proposed consists in selecting the non-dimensionalized high-frequency daily DNI curve which, once transformed back into a dimensional 3-h daily curve, is the closest day in term of Euclidean distance to the DNI 3-h profile of the given input day. This procedure, called *Pattern procedure*, is compared with results obtained by a simple base case forecast procedure. Since the path that solar radiation travels through the atmosphere is not a linear function of time, DNI cannot be a linearly interpolated. In this work, the linear interpolation of the ratio of 3-h input DNI series to 3-h DNI clear sky value is carried out (*Linear procedure*). In order to create this ratio, 1-min clear sky DNI values were calculated using REST-2 clear sky model [5] and summed to 3-h DNI clear sky values.

Data Analysis

A day classification into different categories according to their clearness index, kt (the ratio of GHI to top-of-atmosphere solar irradiance on the same plane), has been carried out. The data recorded were classified in the following daily kt intervals: (<0.3; 0.3-0.4; 0.4-0.5; 0.5-0.6; 0.6-0.7; > 0.7), which were assigned the following nominal values: (<0.30; 0.35; 0.45; 0.55; 0.65; >0.70).

In this work, the following parameters are calculated for the daytime (from sunrise to sunset) for comparing modeled and measured series:

- **Distribution similitude**. The statistical metric used in this work to check the distribution similitude between generated and measured high-frequency DNI values is the KSI (Kolmogorov-Smirnov test Integral) index [6]. This parameter is defined as the integrated differences between the Cumulative Distribution Functions (CDF) of two datasets.
- **Variability**. For quantifying DNI variability, the statistical metrics used in this work is the ramp rate (RR) being calculated from daytime 1-min data. RRs are analyzed as a function of day clarity and location. DNI irradiance under clear sky conditions, DNI^{CS}, is calculated using the REST2 model [5] and is subtracted from the measured and generated DNI, such that the remaining value is a variation from the expected clear-sky irradiance [7]. Thus, the RRs of these variations are calculated as the difference between successive data points over 1-min, using the following equation given in units of W/m^2min (eq. 1):

$$RR = \frac{DNI(t) - DNI^{CS}(t) - \left[DNI(t-1) - DNI^{CS}(t-1)\right]}{\Delta t} \quad (1)$$

RESULTS

Table 2 shows the number of days included in each category analyzed (*n*), the corresponding daily kt mean values (*mean*) and also their standard deviations (*sd*). From this table it can be seen that the standard deviation of daily kt monotonically decreases with increasing mean daily kt classes, indicating lower dispersion at clearer conditions.

TABLE 2. Statistical information for daily kt intervals in each location analyzed.

Daily kt interval	Assigned nominal value	n	mean	sd
0.0 - 0.3	<0.30	155	0.219	0.059
0.3 - 0.4	0.35	104	0.347	0.031
0.4 - 0.5	0.45	136	0.455	0.030
0.5 - 0.6	0.55	224	0.553	0.029
0.6 - 0.7	0.65	586	0.66	0.027
0.7 – 1.0	>0.70	397	0.723	0.014

Figure 2 shows 1-min measured DNI (red) for several day types, as well as the respective 1-min DNI generated through the Linear Interpolation procedure (green). Figure 3 shows the same measured days (red) with the respective 1-min DNI values generated through the Dynamic Path procedure (blue).

The cloudiest day shown in these figures (daily kt = 0.34, 2009/10/22) has measured peaks over 750 W/m^2, and shows rapid transitions between clear and cloud conditions. This dynamic is well represented by the *Pattern* procedure, which reproduces those rapid transitions as well as their maximum values. On the contrary, 1-min DNI generated by *Linear* procedure does not reach too high or zero values, keeping low values and smoothly decreasing when measured DNI peaks are less frequent (and consequently, its 3-h averages decreases). It is worth to highlight that, for this day, the root mean square error (RMSE) is lower for *Linear* (115 W/m^2) than for *Pattern* 1-min DNI generated series (154 W/m^2), with respect to the measured ones. This fact is due to the high differences found between *Pattern* 1-min DNI generated and measured values: peaks in these datasets are not simultaneously, but they can alternate increasing considerably RMSE values. On the contrary, *Linear* generated 1-min DNI series shows a smooth dynamics, passing their values through the measured DNI peaks and minimizing the root square of their differences. With respect to their distributions, *Pattern* generated series shows a lower KSI (4.5%) than *Linear* series (24.6%).

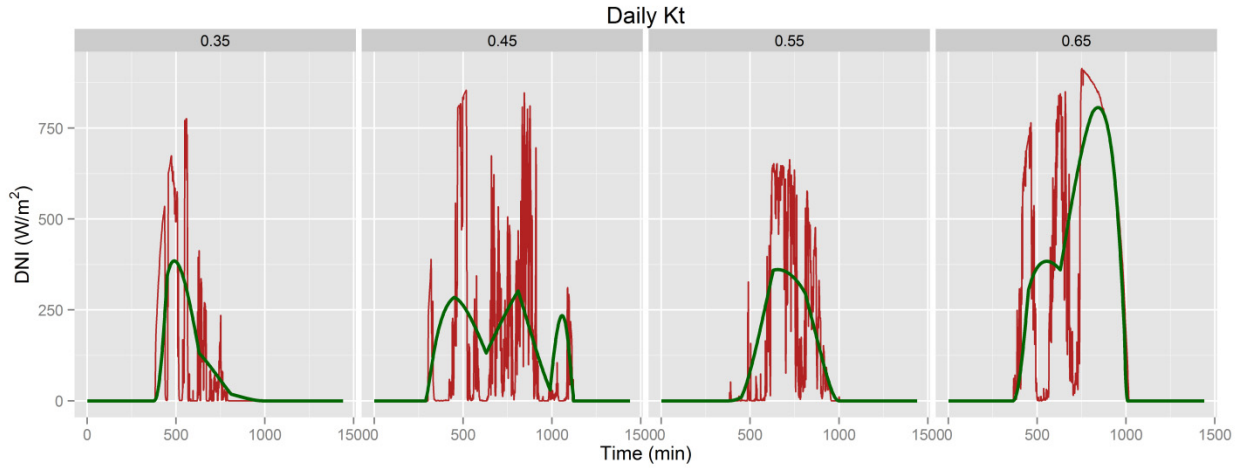

FIGURE 2. Measured (red) and generated by means of *Linear* procedure (green) generated 1-min DNI for different daily kt intervals studied.

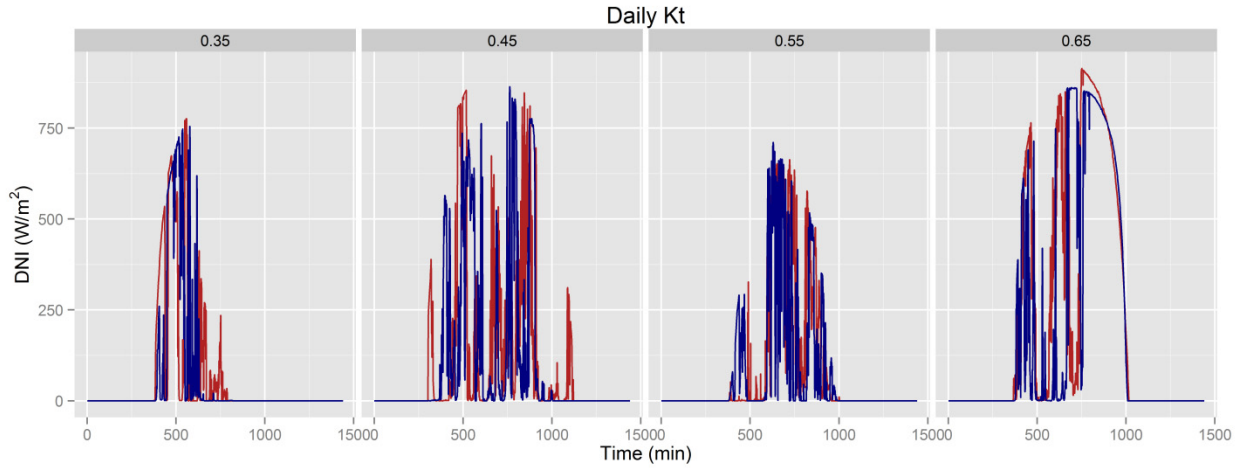

FIGURE 3. Measured (red) and generated by means of *Pattern* procedure (blue) generated 1-min DNI for different daily kt intervals studied.

1-min measured DNI series of intermediate days shown in Fig. 2 and Fig 3 with daily kt of 0.48 and 0.52 (corresponding to 2010/08/12 and 2008/10/18, respectively) shows a similar dynamics than the previous one, with a higher prevalence of clear sky conditions. Again, *Pattern* procedure provides a similar dynamic behavior than measured ones, by generating both peak amplitude and duration similar to those observed. With respect to their distributions, *Pattern* generated series shows a lower KSI (5.6% and 6.2%, respectively) than *Linear* series (129.4% and 40.6%, respectively). RMSE is greater in the *Pattern* generated series (235 W/m^2 and 131W/m^2, respectively) than in *Linear* generated series (171 W/m^{2}and 106 W/m^2, respectively).

In the clearest day shown in Fig. 2 and Fig. 3 (daily kt = 0.62, corresponding to 2009/10/14), it is appreciated a better performance of *Linear* procedure in comparison with previous cases, which roughly follows the highest peak present in measured DNI series. The *Pattern* generated series also detect and reproduce faithfully peaks present in measured series as in previous cases. In this case, RMSE is again lower in the *Linear* generated series (177 W/m^2) than in *Pattern* generated series (243 W/m^2). KSI value is also lower in this *Pattern* generated series (7.3%) than in this *Linear* generated series (15.4%).

Having now discussed single days as examples, statistical results are provided for the full time series period from 2005 to 2011. Table 3 shows KSI values calculated from the comparison of generated and measured 1-min DNI series. *Pattern* generated series keep always KSI values lower than *Linear* generated series, indicating their better similarity with measured distributions. In particular, intermediate day types (daily kt values of 0.45 and 0.55) are well reproduced by this procedure in all the stations analyzed. These cases constitute intermediate days, which normally have enough DNI for CSP generation and frequent passing clouds. It is also worth to mention that *Linear* procedure offers their lower KSI values (below 100%) at daily kt values > 0.70, as expected (over-simplistic forecast procedures can yield very good conventional statistical metrics).

TABLE 3. KSI (%) values of the cases analyzed.

Daily kt	Linear interpolation	Pattern procedure
<0.30	126.3	83.1
0.35	183.6	34.3
0.45	231.0	9.2
0.55	216.7	17.5
0.65	123.1	14.6
>0.70	16.3	8.9

In order to visually examine the similarity of daytime 1-min DNI measured and generated distributions, Fig. 4 shows their empirical cumulative distribution function (ECDF) for the daily kt intervals studied. Measured 1-min DNI ECDF (red lines) in the daily kt < 0.30 case are located at the top left part of the ECDF graph. These days show a high percentage of measured DNI values equal to zero (completely overcast conditions) and maximum measured DNI values are low for these days. At increasing daily kt values, there is a smooth transition of the measured 1-min DNI curve (red), and large DNI values occur more frequently, while the number of low DNI values is decreasing. *Linear* ECDF (green) differs from the measured one in intermediate kt days (0.45 and 0.55), while the *Pattern* ECDF (blue) remains much closer to the measured ECDF. For very clear skies, the *Linear* ECDF again is becoming more similar to the measured ECDF (especially in the case kt > 0.70).

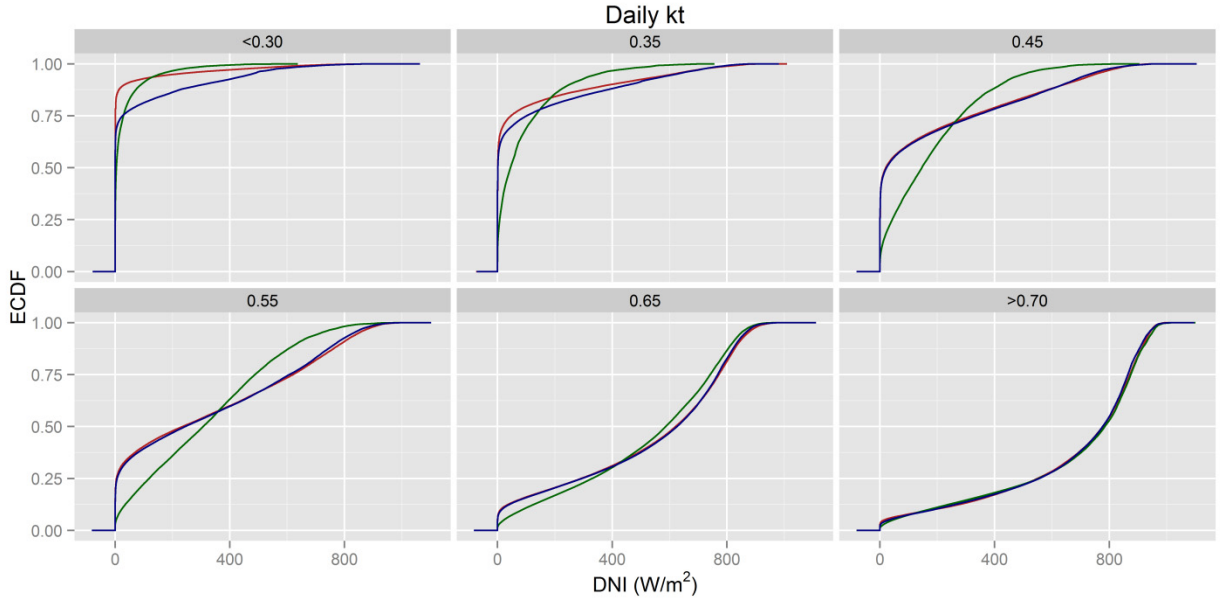

FIGURE 4. ECDF of 1-min measured (red) and generated (*Pattern*, blue; *Linear*, green) 1-min DNI series.

Table 4 shows mean and standard deviation for 1-min DNI Ramp Rates. Very low mean values were found in all cases analyzed, whereas standard deviation is highly dependent on daily kt. The highest standard deviation for measured 1-min DNI RRs are found at intermediate daily kt cases (kt = 0.45 and 0.55), having the extreme day types (kt < 0.30 and kt > 0.70) low standard deviation values and thus reflecting more stable conditions. Ramp Rate standard deviation of *Linear* interpolation series keep low values (<6 W/m^2min), whereas the standard deviation of Ramp Rate calculated from *Pattern* generated series follows a similar trend to that observed in measured series, but with lower values (in a factor of 0.7 approximately).

TABLE 4. Ramp rate mean and standard deviation for 1-min daytime DNI.

Parameter	Daily kt	Measured	Linear interpolation	Pattern procedure
Mean (W/m^2min)	<0.30	0.0	0.0	0.0
	0.35	0.0	0.0	0.0
	0.45	0.0	0.0	0.0
	0.55	0.0	0.0	0.0
	0.65	0.0	0.0	0.0
	>0.70	0.0	0.0	0.0
Standard deviation (W/m^2min)	<0.30	39.6	4.2	34.4
	0.35	63.8	4.1	50.8
	0.45	84.0	5.5	59.7
	0.55	85.1	5.4	58.7
	0.65	63.5	4.6	39.0
	>0.70	40.8	3.8	24.0

CONCLUSIONS

A methodology for generating synthetic DNI time series at 1-min temporal resolution from 3-h DNI input series is presented (*Pattern* procedure), and its performance is compared with a base case consisting of the linear interpolation of the ratio of actual DNI to clear DNI (*Linear* procedure).

The precise minute to minute DNI forecast is an unaffordable task due to the wide variety of high frequency solar irradiance transitions at different solar elevations, day types, hourly averages, its autocorrelation [7, 8] and also its site-dependency [10]. Consequently, in order to properly evaluate and compare high frequency series, it is recommendable to avoid statistical parameters of dispersion that specifically compare point-to-point like RMSE. In this work, it is appreciated that well forecasted daily series (according to KSI, Ramp Rate and visual analysis) obtained by means of the *Pattern* procedure can provide high RMSE values in comparison with the *Linear* procedure which provide non-realistic curves for those days.

In this work we propose the analysis of time series distribution and variability. The results shown in this paper confirm that even the simplistic forecast procedure used as a base case can provide good performance in clear days. Consequently, it is recommended to break down the forecast performance analysis into several categories representing different sky conditions. An intuitive and practical way to perform this classification is using the daily clearness index.

Further work is necessary to compare forecast methodologies in locations belonging to different climate zones, as 1-min solar irradiance series are highly site-dependent. Finally, recent works suggest that this procedure can be also adapted for Global Horizontal solar Irradiance (GHI) forecasts [11].

ACKNOWLEDGMENTS

This project has received funding from the European Union's Horizon 2020 research and innovation programme under grant agreement No 654984. The authors would like also to thank the manager and staff of Carpentras BSRN station for their efforts in establishing and maintaining that stations.

REFERENCES

1. J. Kleissl, *Solar Energy Forecasting and Resource Assessment* (Oxford : Elsevier Ltd., 2013)
2. A. Ohmura, et al., Bulletin of the American Meteorological Society **79**, 2115-2136 (1998).
3. C.M. Fernández Peruchena, M. Blanco, and A. Bernardos, Energy Procedia **49**, 2321-2329 (2014).
4. C.M. Fernández-Peruchena et al, Solar Energy **115**, 255-263 (2015).
5. C.A. Gueymard, Solar Energy **82**, 272-285 (2008).
6. B. Espinar, et al., Solar Energy **83**, 118-125 (2009).
7. M. Lave and J. Kleissl, Renewable Energy **35**, 2867-2873, (2010).
8. H.G. Beyer, et al., "Synthesis of DNI time series with sub-hourly time resolution." In Proceedings of the 16th SolarPACES Conference (Perpignan, France, 2010).
9. T. Tomson and M. Hansen, Est J Eng **16**, 176-183 (2010).
10. C.M. Fernández-Peruchena and A. Bernardos, Solar Energy **112**, 425-436 (2015).
11. C.M. Fernández-Peruchena, et al., Renewable Energy **86**, 375-383 (2016).